# Task-driven intra- and interarea communications in primate cerebral cortex

Adrià Tauste Campo[a], Marina Martinez-Garcia[a,b,c], Verónica Nácher[d], Rogelio Luna[d], Ranulfo Romo[d,e,1], and Gustavo Deco[a,f]

[a]Center for Brain and Cognition, Department of Information and Communication Technologies, Universitat Pompeu Fabra, 08018 Barcelona, Spain; [b]Department of Ophthalmology and [c]Institute of Neuropathology, RWTH Aachen University, 52076 Aachen, Germany; [d]Instituto de Fisiología Celular-Neurociencias, Universidad Nacional Autónoma de México, 04510 Mexico D.F., Mexico; [e]El Colegio Nacional, 06020 Mexico D.F., Mexico; and [f]Institució Catalana de Recerca i Estudis Avançats, 08010 Barcelona, Spain

Contributed by Ranulfo Romo, March 1, 2015 (sent for review June 1, 2014; reviewed by Stefano Panzeri and Rodrigo Quian Quiroga)

**Neural correlations during a cognitive task are central to study brain information processing and computation. However, they have been poorly analyzed due to the difficulty of recording simultaneous single neurons during task performance. In the present work, we quantified neural directional correlations using spike trains that were simultaneously recorded in sensory, premotor, and motor cortical areas of two monkeys during a somatosensory discrimination task. Upon modeling spike trains as binary time series, we used a nonparametric Bayesian method to estimate pairwise directional correlations between many pairs of neurons throughout different stages of the task, namely, perception, working memory, decision making, and motor report. We find that solving the task involves feedforward and feedback correlation paths linking sensory and motor areas during certain task intervals. Specifically, information is communicated by task-driven neural correlations that are significantly delayed across secondary somatosensory cortex, premotor, and motor areas when decision making takes place. Crucially, when sensory comparison is no longer requested for task performance, a major proportion of directional correlations consistently vanish across all cortical areas.**

vibrotactile discrimination | large-scale cortical networks | spike-train analysis | information theory | decision making

The problem of neural communication in the brain has been little explored traditionally due to the need for simultaneous recordings (1). The arrival of new techniques to record both neural population activity and single-neuron action potentials offers new prospects to study this problem (2, 3). Recently, population recordings have motivated a large number of works on multiunit interactions, including the study of interactions between local field potentials (LFPs) (4–6), LFPs and multiunit activity (5), and LFPs and neuronal spikes (7), but less attention has been paid to interactions between single-unit recordings (8). However, the analysis of simultaneous spike trains becomes critical because it is generally assumed that neurons are key units in distributing information across brain areas (9).

An ideal paradigm to study neural communication is the somatosensory discrimination task designed by Romo and coworkers (10). In this task, a trained monkey discriminates the difference in frequency between two mechanical vibrations delivered sequentially to one fingertip (Fig. 1*A*). Essentially, the monkey must hold the first stimulus frequency ($f1$) in working memory, must compare the second stimulus frequency ($f2$) with the memory trace of $f1$ to form a decision of whether $f2 > f1$ or $f2 < f1$, and must postpone the decision until a sensory cue triggers the motor report (11). At the end of every trial, the monkey is rewarded with a drop of liquid for correct discriminations. Previous work on this task has analyzed how single-neuron responses across sensory and motor areas linearly correlate with stimuli and the decision report during the key stages of the task (12). The results show that stimuli are mostly encoded in somatosensory areas, the processes of working memory; that comparison takes place in the secondary somatosensory cortex (S2) and premotor areas; and that behavioral information is primarily found in premotor and motor areas. Thus, the somatosensory discrimination task activates complex processes that are required to communicate information from the areas that encode the stimuli to the areas that integrate them and report the decision.

In the present work, we study this communication paradigm through the analysis of simultaneous recordings of neurons engaged in the task (6, 13) from two monkeys. Indeed, by applying nonlinear statistical methods, we estimate modulated cortical correlations that help describe how task-related information flows from sensory to motor areas when a correct decision is made.

## Results

We studied interactions between neuronal spike trains that were simultaneously recorded from five cortical areas in one trained monkey performing a somatosensory discrimination task (6). Recordings for the first monkey were performed in 13 independent sessions ($n = 13$). During each session, up to seven microelectrodes were individually inserted in each of the five cortical areas for simultaneous recordings of single neurons. The selected neurons were from two somatosensory areas, primary somatosensory cortex (S1) and S2, and three premotor/motor areas, medial premotor cortex (MPC), dorsal premotor cortex (DPC), and primary motor cortex (M1) (*Materials and Methods*). To investigate neural correlations during the discrimination task, we only considered correct ("hit") trials of similar psychophysical performance. We validated our results by repeating the same analysis on a second trained monkey in 19 sessions divided into two block of three simultaneously recorded areas each (S1, S2, and DPC and S1, S2, and M1).

The central measure of our analysis is the directed information (DI), mathematically denoted by $I(X^T \to Y^T)$, which is a nonlinear

### Significance

**How do multiple neurons communicate to solve a cognitive task? To answer this question, we investigate spike-train directional correlations across five primate cortical areas simultaneously recorded during a somatosensory discrimination task. Correlations are inferred using a nonparametric procedure that models spike trains as Markovian binary series and dynamically estimates the directed information between every neuron pair at different delays. We find that information processing during the discrimination task can be described by intra- and interarea decision-driven delayed correlations, which are no longer found when a monkey receives both stimuli but does not perform the task.**

Author contributions: A.T.C., M.M.-G., V.N., R.L., R.R., and G.D. designed research, performed research, analyzed data, and wrote the paper.

Reviewers: S.P., Italian Institute of Technology; and R.Q.Q., University of Leicester.

The authors declare no conflict of interest.

[1]To whom correspondence should be addressed. Email: rromo@ifc.unam.mx.

This article contains supporting information online at www.pnas.org/lookup/suppl/doi:10.1073/pnas.1503937112/-/DCSupplemental.

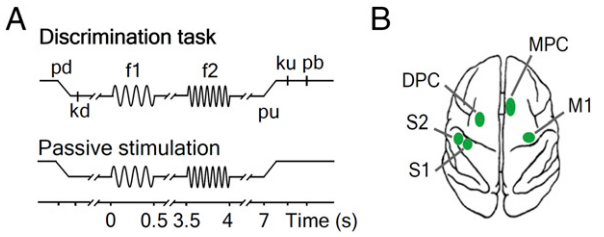


**Fig. 1.** Somatosensory discrimination task and cortical recording sites. (*A*) Sequence of events during the discrimination and passive stimulation tasks (f1, first stimulus; f2, second stimulus; kd, key down; ku, key up; pb, push-button; pd, probe down; pu, probe up) (*Materials and Methods*). (*B*) Top view of the monkey brain and the recorded cortical areas (green spots).

measure of directional correlation between the processes $X^T$ and $Y^T$ (14). When the two process are identical (i.e., $X^T = Y^T$), this measure coincides with the Shannon entropy, denoted by $H(Y^T)$ (15). The DI $I(X^T \to Y^T)$ quantifies for any given time $t$ the information that the past and present of $X^T$ (up to time $t$) has about the present of $Y^T$ upon the knowledge of the past of $Y^T$ (up to time $t-1$). Alternatively, the entropy of $Y^T$ quantifies the uncertainty on any realization of $Y^T$.

**Neural Correlations Are Task-Driven.** We estimated the entropy in 870 neurons and the DI in 50,616 ordered neuron pairs from two monkeys to infer significant auto- and pairwise directional correlations across time delays of $0, 10, 20, \ldots, 140$ ms and during 17 consecutive task intervals of 0.5 s, spanning from the interval before the $f1$ stimulation to the interval after the lift of the sensory cue. This cue lift interval will hereafter be referred to as the probe-up (*pu*) period (Fig. 1*A* and *Materials and Methods*).

In particular, for every task interval, we tested the significance of each estimated measure against a null hypothesis of complete directional independence using the maximum value of the DI over all selected delays as a test statistic (*Materials and Methods*). First, we selected every neuron whose entropy was significant (permutation test, $\alpha = 5\%$) for at least one of the frequency pairs and denoted it a "responsive neuron." In a similar vein, every significant correlation between responsive neurons for at least one of the frequency pairs was denoted a "responsive path," and each correlated neuron was denoted either a "starting point" or "end point" neuron according to the correlation's directionality. Conversely, every path whose starting point/end point was a given neuron was denoted an "outgoing/incoming" path to that neuron, respectively (*SI Appendix*, section 2). For every interarea comparison, we computed the percentage of responsive paths over all possible simultaneous pairs. For instance, *SI Appendix*, Fig. S1 shows that responsive paths in the first monkey were found above significance level ($\alpha' = 9.75\%$) across all area pairs and task intervals (green curves).

We studied whether responsive paths were directly associated with the discrimination task. To this end, we estimated again the directional correlation in every neuron pair that formed a responsive path during a control task, in which the monkey received identical mechanical vibrations but was requested to remain still upon a reward that arrived at variable time (passive stimulation; Fig. 1*A* and *Materials and Methods*). Under passive stimulation, only a small fraction of the responsive paths were again found significant ($\approx 20\%$) across all area pairs and task intervals (gray curves, *SI Appendix*, Fig. S1). Overall, there was a low correlation between the presence of responsive paths during the original task and the control task in both monkeys [$\rho < 0.03$, Spearman correlation (16)], suggesting that neural correlations were driven by weakly dependent processes.

We then wondered whether both tasks were also differentiated by single-neuron measures under fixed stimulation. To examine this question, we focused on the ensemble of neurons that were end point neurons of responsive paths and measured their activity during each task. First, we measured the firing rate and spike-train entropy of every neuron in the ensemble. Then, as a benchmark multineuron measure, we evaluated the aggregated sum of DI along every neuron's incoming responsive paths. For the first monkey, Fig. 2 shows the average firing rate, average entropy, and average incoming DI during both tasks when $(f1 = 14, f2 = 22)$ Hz, together with their error bars. Neurons exhibited consistent single-neuron differences across tasks in MPC, DPC, and M1 around $f2$ stimulation.

In contrast, the use of directional correlations shows that in those periods when neurons were equally firing in both tasks (or with similar spike-train entropies), they were less influenced through responsive paths during passive stimulation than during somatosensory discrimination. Results were similar for the frequency pair $(f1 = 30, f2 = 22)$ Hz (*SI Appendix*, Fig. S2) and were also corroborated in a second monkey (*SI Appendix*, Fig. S7).

**Neural Correlations Are Modulated by Decision Making.** Despite being task-driven, the role of responsive paths still remained unclear because they were uniformly present across all areas and task intervals (*SI Appendix*, Fig. S1). In particular, to what extent were these paths communicating task-related information?

To investigate more intrinsic connections between neural correlations and decision making, we searched for the subset of responsive paths that were significantly modulated by a key task variable. More precisely, we tested the modulation of every responsive neuron and path with respect to the decision sign $D = f1 - f2$ by computing the difference between the DI estimates across trials recorded at frequency pairs $(f1 = 14,\ f2 = 22)$ Hz $(D < 0)$ and $(f1 = 30, f2 = 22)$ Hz $(D > 0)$. Responsive neurons and paths that were significantly modulated (permutation test, $\alpha = 5\%$) were thus denoted as "modulated neurons" and "modulated paths,"

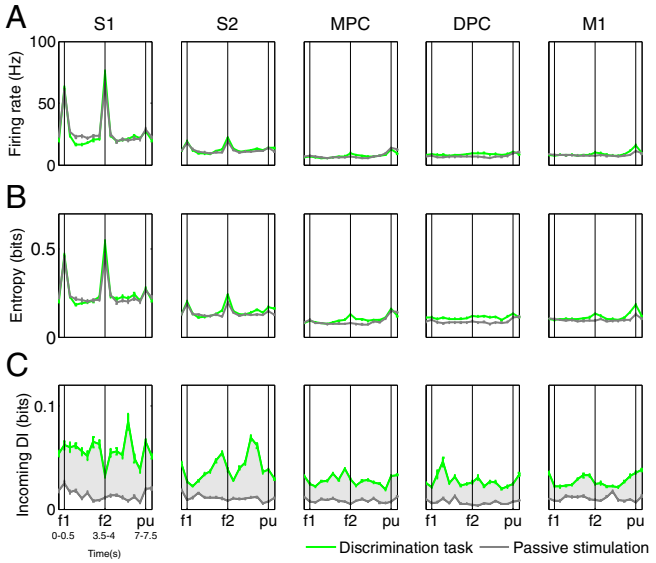


**Fig. 2.** Single-neuron vs. multiple-neuron measures in the first monkey. Comparison between discrimination (green) and passive stimulation (gray) tasks across areas using the average value of distinct measures over the ensemble of neurons with incoming responsive paths. Data were obtained in 13 sessions ($n = 13$) from areas S1, S2, DPC, MPC, and M1, and are plotted for 17 consecutive intervals when $f1 = 14$ Hz and $f2 = 22$ Hz. Vertical bars outline the intervals $f1$ and $f2$ and the *pu* period. Error bars (±2 SEM) denote the SD of the sample mean. (*A*) Average firing rate. (*B*) Average entropy. (*C*) Average (across the ensemble of neurons) sum of DI along incoming responsive paths. The shadowed gray area indicates the difference of this measure between both tasks.

respectively. By this choice of trials, modulated paths have a different interpretation depending on the task interval. For instance, during the intervals before $f2$ stimulation, modulations can be regarded as correlates of $f1$, whereas during the intervals after $f2$ stimulation, they can be interpreted as correlates of the decision sign and the associated motor action. Green curves in Fig. 3 and *SI Appendix*, Fig. S3 show the percentage of modulated neurons (Fig. 3*A*) and modulated paths (Fig. 3*B* and *SI Appendix*, Fig. S3) while the first monkey was performing the discrimination task, and black circles indicate the intervals when this percentage was significantly [Agresti–Coull confidence interval (17), $\alpha = 5\%$] above chance level ($\alpha = 5\%$). In the rest of this article, we will use this statistical sense when referring to percentages that are above significant level. Area comparisons in Fig. 3 were chosen to describe the chain of comparisons S1 ↔ S2 ↔ MPC ↔ DPC ↔ M1. In general, Fig. 3 and *SI Appendix*, Fig. S3 show that the directional measure was able to discriminate top-down from bottom-up interactions in each recorded area pair.

Because both modulated neurons and paths carried task information, we analyzed their mutual relationship by computing the proportion of modulated paths that linked modulated neurons. In contrast to responsive paths, modulated neurons were positively correlated with the presence of their own outgoing or incoming modulated path in both monkeys (Spearman correlation; *SI Appendix*, Figs. S4*A* and S9*A*), which implied that the proportion of modulated paths linking modulated neurons was above chance level for every area and during the majority of task intervals (first monkey; *SI Appendix*, Fig. S4*B*). This preliminary result indicates that modulated paths were prone to link modulated neurons.

Fig. 3 and *SI Appendix*, Fig. S3 illustrate how sensory information was encoded and distributed from sensory to motor areas in the first monkey while the percept was processed to drive a motor action. On one hand, S1 encoded $f1$ at the first stimulation period and was especially active in distributing this information toward S2, MPC, and M1 during working memory intervals (Fig. 3 and *SI Appendix*, Fig. S3). On the other hand, S1 was interactive with premotor and motor areas around the *pu* period, which suggests that the sensory cue delivered at the *pu* period produced sensory-motor correlations that could anticipate the report (*SI Appendix*, Fig. S3). Neurons from S2 received sensory information from S1 and MPC during the interstimulus interval (Fig. 3*B*) but did not individually encode it (Fig. 3*A*). This lack of local activity after $f1$ stimulation may be a consequence of S2's function in encoding and integrating $f2$ (12), whose value was kept fixed in our study. The role of MPC was to mediate between sensory and motor areas in two different stages. First, during the intervals before $f2$ stimulation, MPC received incoming interactions from sensory areas that were modulated by $f1$ (Fig. 3*B* and *SI Appendix*, Fig. S3). Second, during the postponed decision, MPC mainly produced outgoing interactions to M1 and to other neurons within MPC that were modulated by the decision sign (*SI Appendix*, Fig. S3). Neurons from DPC showed heterogeneous communication patterns with respect to sensory areas and MPC. However, a great proportion of them received task information by persistent links from M1. The area M1 exhibited two distinct roles while communicating with the rest of cortical areas. First, it was influenced by S1 and S2 around $f2$ stimulation, which indicates that there was an information link between sensory and motor areas regardless of the encoding patterns found in each area (Fig. 3*A* and *SI Appendix*, Fig. S3).

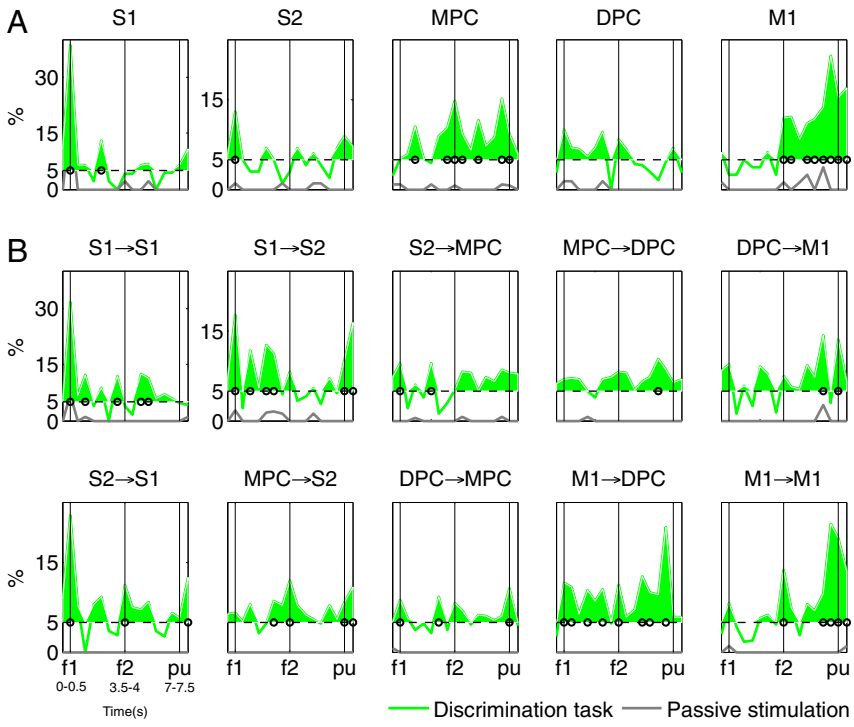


**Fig. 3.** Modulated neurons and paths in the first monkey. Percentages during the discrimination task are shown in green. Percentages during passive stimulation are shown in gray. Arrows in the titles indicate the directionality of the modulated paths. Vertical bars outline the intervals $f1$ and $f2$ and the *pu* period. Horizontal dashed lines indicate significance level ($\alpha = 5\%$). The shadowed green area indicates the percentages of modulated paths above significance level. Black circles indicate the intervals when the estimated percentage was significantly different [Agresti–Coull confidence interval (17), $\alpha = 5\%$] from significance level. (*A*) Percentage of modulated neurons over all responsive neurons in each recorded area. (*B*) Percentage of modulated paths over all responsive paths in 10 intra- and interarea comparisons. Data were obtained in 13 sessions ($n = 13$) from areas S1, S2, DPC, MPC, and M1, and are plotted for 17 consecutive intervals.

Second, M1 was highly interactive with the rest of premotor and motor areas in the process of conforming the decision and the motor action in line with previous results (12). The pattern of intraarea activity of M1 peaked at *f2* stimulation and near the *pu* period, which indicates that these events were the main drivers of local information exchange.

In contrast, during passive stimulation, neither modulated neurons nor modulated paths were generally associated with $f1$ and the monkey's choice. Modulated neurons and paths only showed some persistency in S1 during the first stimulation (gray curves, Fig. 3), which confirms the existence of minimal sensory processing in S1 during the control task (12). This abrupt change in the activity of modulated neurons and paths was corroborated in a second monkey (*SI Appendix*, Fig. S8).

**Task-Specific Delayed Correlations Distribute Sensory and Behavioral Information.** We further studied interarea communications by analyzing two characteristics of modulated paths: their modulation rule and their correlation delay. First, we divided modulated paths into three classes: ON-ON, defined to involve significant correlations in both decision signs, and ON-OFF and OFF-ON, defined to be significant only for $f1 < f2$ and $f1 > f2$, respectively. The majority of modulated paths in both monkeys were of the form ON-OFF and OFF-ON (Fig. 4*A* and *SI Appendix*, Fig. S9*B*), indicating that task information was mainly encoded by the presence of significant correlations during trials of one decision report that vanished during trials of the opposite decision report. The almost equal contribution of ON-OFF and OFF-ON modulations along the task gave rise to an overall picture that was difficult to interpret (*SI Appendix*, Fig. S5). To observe how these modulations interplayed for a specific interarea comparison in the first monkey, Fig. 4*B* shows the percentage of modulation classes above significant level ($\alpha = 5\%$) and Fig. 4*C* shows the sum of the average (across trials) DI along modulated paths starting at M1 and ending at DPC in each decision report. Fig. 4 *B* and *C* also highlight the three stages where the aggregated DI peaked (time periods and corresponding values in dashed rectangles). These stages may be linked to the acquisition of $f1$ (intervals 2 and 3), the recovery of $f1$ before the comparison takes place (interval 9), and the process of planning the action (interval 15). Comparison of both figures at the later stage shows that a similar number of sign-specific paths could lead to twice as much aggregated DI for one decision report than for the opposite decision report.

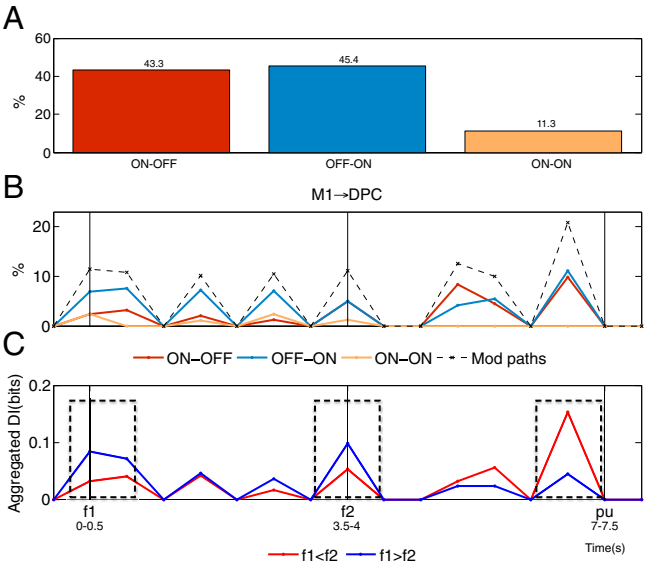


**Fig. 4.** Modulation classes during the discrimination task in the first monkey. (*A*) Distribution of modulated paths from intervals above significant level ($\alpha = 5\%$) into the classes ON-OFF, OFF-ON, and ON-ON. (*B*) For the comparison M1-DPC, percentage of modulation classes during task intervals above significant level: percentages of ON-OFF modulations (significant only for $f1 < f2$, red), percentages of OFF-ON modulations (significant only for $f1 > f2$, blue), and percentages of ON-ON modulations (significant for both decision reports, orange). For reference, the total percentage of modulated paths is plotted in a dashed black line with cross markers. (*C*) Aggregated sum of the average (across trials) DI along modulated paths from M1 to DPC during task intervals above significant level for the decision reports ($f1 = 14$ Hz, $f2 = 22$ Hz), ($f1 < f2$, red) and ($f1 = 30$ Hz, $f2 = 22$ Hz), ($f1 > f2$, blue). In *B* and *C*, arrows in the title indicate the directionality of the modulated paths. Vertical bars outline the intervals $f1$ and $f2$ and the *pu* period. Data were obtained in 13 sessions ($n = 13$) from areas S1, S2, DPC, MPC, and M1, and are plotted in *B* and *C* for 17 consecutive intervals.

To study interneuronal delays, we divided the modulated paths that were found above significant level in the first monkey into three sets according to their estimated delays: 0 ms, $[10, 70]$ ms, and $[80, 140]$ ms. The interneuronal interactions at these delays were computed over a correlation memory of 4 ms (*Materials and Methods*), thus capturing effects additional to those effects found using classical synchronization measures (18). We first plotted the distribution of delays across area pairs and task intervals where modulated paths were above significant level (*SI Appendix*, Fig. S6; $\alpha = 5\%$). We summarized these findings in Fig. 5 after having classified interneuronal delays according to the function (somatosensory/premotor/motor) and location (right/left hemisphere) of each area under comparison. Overall, modulated paths across somatosensory areas were dominated by instantaneous interactions, whereas modulated paths involving premotor and motor areas were mostly delayed at the range of $[80 - 140]$ ms (Fig. 5*A*). In particular, we tested the average delay across area pairs and obtained significant differences [Fig. 5*B*; Wilcoxon test (16), $p < 0.005$] between somatosensory interactions (43.6 ms); interactions between S1 and MPC, DPC, and M1 (64.2 ms); and interactions across S2, MPC, DPC, and M1 (73.4 ms). These differences also emerged after removing the contribution of instantaneous correlations but were no longer significant [Fig. 5*C*; Wilcoxon test (16), $p > 0.05$]. Further, a closer look at *SI Appendix*, Fig. S6 reveals that modulated paths within the somatosensory cortex and within M1 were less delayed than interactions across premotor and motor areas. These findings suggested that differences in the average delay could be driven by the relative location of the areas in the two hemispheres. Then, we computed the average delay across areas within a hemisphere and across areas from distinct hemispheres, obtaining significant differences that were robust to the effect of intraarea correlations [Fig. 5*B*; Wilcoxon test (16), $p < 0.005$]. However, this delay difference did not remain significant after removing the effect of instantaneous correlations [Fig. 5*C*; Wilcoxon test (16), $p > 0.05$]. In sum, instantaneous correlations were key to discriminate interarea relationships with respect to the areas' location and function.

## Discussion

Using nonparametric estimation of spike-train interdependencies, we have unraveled neural correlation paths that are specific to a discrimination task. These paths are task-driven for two main reasons. First, they dramatically decrease when the monkey receives both stimuli but is not requested to perform the cognitive task (Fig. 2). Second, they are modulated in a significant percentage by sensory and behavioral variables (Fig. 3). More importantly, these modulated paths are related to neurons that individually encode task variables and are therefore likely to distribute their information further across other areas (*SI Appendix*, Fig. S4). In general, the use of directional correlations seems to discriminate the original task from a control task better than single-neuron measures (Fig. 2*A*), suggesting that task-driven correlations may not generally be rate-dependent (19).

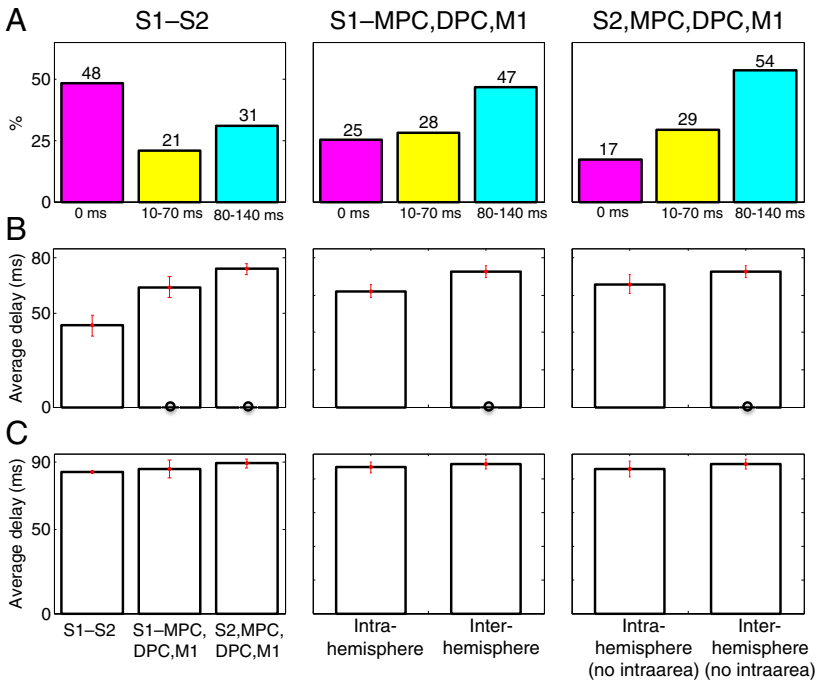


**Fig. 5.** Interneuronal delays during the discrimination task in the first monkey. (*A*) Distribution of modulated path delays at intervals above significant level ($\alpha = 5\%$) into 0 ms (magenta), 10 – 70 ms (yellow), and 80 – 140 ms (cyan) in correlations across S1 and S2 (*Left*); correlations between S1 and MPC, DPC, and M1 (*Center*); and correlations across S2, DPC, MPC, and M1 (*Right*). (*B* and *C*, *Left*) Average delay of aforementioned correlations across S1 and S2; correlations between S1 and MPC, DPC, and M1; and correlations across S2, DPC, MPC, and M1. (*B* and *C*, *Center*) Average delay of correlations across areas within the same hemisphere ("intrahemisphere") and across areas from opposite hemispheres ("interhemisphere"). (*B* and *C*, *Right*) Average delay of correlations across areas within the same hemisphere excluding correlations within the same area ("intrahemisphere no intraarea") and across areas from opposite hemispheres. Error bars in red (±SEM) denote the SD of the delays. Black circles indicate that the difference against the leftmost category was significant (Wilcoxon test, $\alpha = 5\%$). (*B*) Average delay of modulated paths. (*C*) Average delay of noninstantaneous modulated paths. Data were obtained in 13 sessions ($n = 13$) from areas S1, S2, MPC, DPC, and M1.

Modulated paths can be used to characterize the role of each area in distributing relevant information to solve the task (11, 12). In particular, we observed that S1 is particularly important in feed-forwarding sensory information to superior areas, S2 interacts with MPC during the working memory stage, MPC acts as a relay node between sensory and motor areas, and the interactions across MPC ↔ M1 → DPC concentrate the information on the monkey's choice (Fig. 3 and *SI Appendix*, Fig. S3). Modulated paths mainly encode task information by the existence (ON) and absence (OFF) of a given neural correlation, which in particular indicates that each decision is distributed across areas through a different subset of interactions (Fig. 4). For each decision report, modulation paths are delayed according to the hemisphere location and function of each area under comparison. In particular, modulated paths are significantly faster when they distribute information across somatosensory areas (S1 and S2) during intervals before the $f2$ stimulation than when they link S2, premotor, and motor areas during decision making. These findings indicate that sensory and behavioral information may be communicated at different time scales.

Our description of modulated paths in primate cerebral cortex extends beyond previous works in which task-related activity was found to be highly distributed across areas and time intervals (12). To encompass both sets of results, we make hypotheses in two related directions. On the one hand, our analysis of modulation paths suggests that task-related information is jointly encoded by neurons that often do not exhibit individual modulations. On the other hand, the great percentage of responsive paths that are not modulated indicates that there is context-dependent activity beyond encoding of sensory and behavioral variables ($f1$, $f2$, and decision). This activity may be the result of internal processes involving sensory and motor areas, such as arousal, attention, or motivation (20), whose encoding patterns could not be captured with this experimental paradigm. The study of these hypotheses may shed light on the underlying mechanisms that encode, distribute, and transform the required information to solve a cognitive task.

## Materials and Methods

This study was performed on two adult male monkeys (*Macaca mulatta*) weighing 8–12 kg. All procedures followed the guidelines of the National Institutes of Health and Society for Neuroscience. Protocols were approved by the Institutional Animal Care and Use Committee of the Instituto de Fisiología Celular.

**Recordings.** Data acquisition, amplification, and filtering have been described in detail (13). In brief, the activity of single neurons was simultaneously recorded with an array of seven independent, movable microelectrodes (1–1.5 MΩ) inserted in each of five cortical areas. Electrodes within an area were spaced 305 or 500 μm apart (21). Spike sorting was performed manually online, and single neurons were selected if they responded to any of the different components of the discrimination task. In particular, neurons from area S1 had cutaneous receptive fields with quickly adapting properties, whereas neurons from area S2 had large cutaneous receptive fields with no obvious submodality properties. Neurons of the frontal cortex had no obvious cutaneous or deep receptive fields; they were selected if they responded to any of the different components of the discrimination task (12, 13). The cortical areas were S1, S2, MPC, DPC, and M1 (Fig. 1*B*). Recordings in S1, S2, and DPC were made in the hemisphere contralateral to the stimulated hand (left hemisphere), and recordings in MPC and M1 were made contralateral to the responding hand/arm (right hemisphere).

**Discrimination Task.** The paradigm used here has been described (10, 11). The monkey sat on a primate chair with its head fixed in an isolated, soundproof room. The right hand was restricted through a half-cast and kept in a palm-up position. The left hand operated an immovable key (elbow at ~90°), and two pushbuttons were located in front of the animal, 25 cm away from the shoulder and at eye level. The centers of the switches were located 7 cm and

10.5 cm to the left of the midsagittal plane. In all trials, the monkey first placed the left hand and later projected to one of the two switches. Stimuli were delivered to the skin of the distal segment of one digit of the right, restrained hand via a computer-controlled stimulator (2-mm round tip; BME Systems). The initial probe indentation was 500 μm. Vibrotactile stimuli were trains of short mechanical pulses. Each of these pulses consisted of a single-cycle sinusoid lasting 20 ms. Stimulus amplitudes were adjusted to equal subjective intensities; for example, 71 μm at 12 Hz and 51 μm at 34 Hz (a decrease of ~1.4% per hertz). During discrimination trials (Fig. 1*A*), the mechanical probe was lowered (probe down), indenting the glabrous skin of one digit of the hand; the monkey placed its free hand on an immovable key (key down); after a variable prestimulus delay (0.5 – 3 s), the probe oscillated vertically at *f*1; after a fixed delay (3 s), a second mechanical vibration was delivered at *f*2; after another fixed delay (3 s), the probe was lifted off from the skin (*pu* period); and the monkey released the key (key up) and pressed either a lateral or medial pushbutton to indicate whether *f*2 was of higher or lower frequency than *f*1, respectively. The monkey was rewarded with a drop of liquid for correct discriminations. The experimental sets of frequency pairs used during the discrimination task were the same as in a study by Hernández et al. (12) for both monkeys.

**Control Tests.** During a passive stimulation condition, the monkey was trained to maintain its free arm motionless during the trial (Fig. 1*B*). Stimuli were delivered to the fingertip, and the animal remained alert by being rewarded with drops of liquid at different times, but no motor response with the free hand was required.

**Data Analysis.** Data were analyzed offline by using custom-built MATLAB code (MathWorks). We selected 13 experimental sessions from the first monkey and 19 experimental sessions from the second monkey according to the following criteria. First, we selected sessions in which the monkey had similar psychophysical thresholds (10). Second, our analysis required the existence of passive stimulation sessions registered on the population. We estimated neural directional correlations between every neuron pair within a population using a nonparametric estimator of the DI between a pair of discrete time series that were assumed to be generated according to a Markovian process (22). In more specific terms, for a pair time series $(x_1^T, y_1^T)$ of length $T$, where $x_1^T = (x_1, \ldots, x_T)$ and $y_1^T = (y_1, \ldots, y_T)$; a time delay $\delta \geq 0$; and Markovian orders equal to $D_1 > 0$ and $D_2 > 0$, respectively, the DI between the stationary processes of $x_1^T$ and $y_1^T$ (i.e., $\mathcal{X}$ and $\mathcal{Y}$) is estimated through the formula

$$\hat{I}_\delta(\mathcal{X} \to \mathcal{Y}) \triangleq \frac{1}{T} \sum_{t=1}^{T} \sum_{y_t} \hat{P}\left(Y_t = y_t | X_{t-\delta-D_2}^{t-\delta} = x_{t-\delta-D_2}^{t-\delta}, Y_{t-D_1}^{t-1} = y_{t-D_1}^{t-1}\right) \times \log \frac{\hat{P}\left(Y_t = y_t | X_{t-\delta-D_2}^{t-\delta} = x_{t-\delta-D_2}^{t-\delta}, Y_{t-D_1}^{t-1} = y_{t-D_1}^{t-1}\right)}{\hat{P}\left(Y_t = y_t | Y_{t-D_1}^{t-1} = y_{t-D_1}^{t-1}\right)}, \quad [1]$$

where the probability distribution of $(X_1^T, Y_1^T)$ is estimated using the context-tree weighting (CTW) algorithm (23). Eq. **1** quantifies the information that the past of $X_1^T$ at delay $\delta$ (i.e., $X_{t-\delta-D_2}^{t-\delta}$) has about the present of $Y_1^T$ ( i.e., $Y_t$), given the most recent past of $Y_1^T$ (i.e., $Y_{t-D_1}^{t-1}$). This estimator is consistent as long as $(\mathcal{X}, \mathcal{Y})$, the two neuronal time series, form a jointly stationary, irreducible, aperiodic, finite-alphabet Markov process whose order does not exceed the prescribed maximum tree depth in the CTW algorithm (theorem 3 of ref. 22). Before estimating the DI, we preprocessed our data as follows. For a fixed stimulation pair, we first binarized spike-train trials using bins of 2 ms (mapping 1 to each bin with at least one spike and 0 otherwise). We then divided each time series into 17 consecutive task intervals of 0.5 s (250 bins). For each neuron, segments that corresponded to the same type of trials and task interval were assumed to be generated by a common random process that satisfied the estimator requirements with a maximum memory of 4 ms ($D_1 = D_2 = 2$ bins) for both the joint and the marginal spike-train processes. Under this assumption, it can easily be checked that the DI is asymptotically equivalent to the transfer entropy (24) in the limit of the time-series length. To assess that neurons were able to express information through their spike-train responses, we run the estimator of the entropy (a particular case of the DI estimator) for each neuron and task interval over the time series that resulted from the concatenation of the fixed stimulation trial segments. Finally, among those neurons that had a significant entropy value, we run the DI estimator (*SI Appendix*, section 3) over all possible simultaneous neuron pairs across delays of 0, 10, 20, 30, 40 ,50, 60, 70, 80, 90, 100, 110, 120 ,130, 140 ms, where the total range was chosen to be compatible with the latency of each area (11, 25) (*SI Appendix*, section 4).

To assess the statistical significance of the estimations, we used a Monte Carlo permutation test (26), where the original (i.e., nonpermuted) results were compared with the tail of a distribution obtained by permuting 20-fold the concatenations of the second binarized spike train $Y^T$ differently for each original estimation ($\alpha = 5\%$) and computed the corresponding $P$ value (27). We dealt with the multiple-test problem (one test for each delay) by using the maximum DI over all selected delays as a test statistic. Further details about the significance analysis for the DI computations and the modulation tests are provided in *SI Appendix*, section 5.

**ACKNOWLEDGMENTS.** R.R.'s research was partially supported by International Research Scholars Award 55005959 from the Howard Hughes Medical Institute, Dirección de Personal Académico de la Universidad Nacional Autónoma de México Grant IN203210, and Consejo Nacional de Ciencia y Tecnología Grant CB-2009-01-130863. V.N. was supported by a Ministerio de Educación y Ciencia-Fullbright Postdoctoral Fellowship from the Spanish Ministry of Science and Technology and Dirección de Personal Académico de la Universidad Nacional Autónoma de México. Support for this work was provided by European Project FP7-ICT BrainScales (G.D. and M.M.-G). In addition, G.D. was supported by the European Research Council Advanced Grant DYSTRUCTURE (Grant 295129) and by the Spanish Research Project SAF2010-16085. A.T.C. was supported by the European Community's Seventh Framework Programme (FP7/2007-2013) under Grant Agreement PEOPLE-2012-IEF-329837.

1. Salinas E, Sejnowski TJ (2001) Correlated neuronal activity and the flow of neural information. *Nat Rev Neurosci* 2(8):539–550.
2. Brown EN, Kass RE, Mitra PP (2004) Multiple neural spike train data analysis: State-of-the-art and future challenges. *Nat Neurosci* 7(5):456–461.
3. Buzsáki G (2004) Large-scale recording of neuronal ensembles. *Nat Neurosci* 7(5):446–451.
4. Roelfsema PR, Engel AK, König P, Singer W (1997) Visuomotor integration is associated with zero time-lag synchronization among cortical areas. *Nature* 385(6612):157–161.
5. Womelsdorf T, et al. (2007) Modulation of neuronal interactions through neuronal synchronization. *Science* 316(5831):1609–1612.
6. Nácher V, Ledberg A, Deco G, Romo R (2013) Coherent delta-band oscillations between cortical areas correlate with decision making. *Proc Natl Acad Sci USA* 110(37):15085–15090.
7. Koralek AC, Costa RM, Carmena JM (2013) Temporally precise cell-specific coherence develops in corticostriatal networks during learning. *Neuron* 79(5):865–872.
8. Hoffman KL, McNaughton BL (2002) Coordinated reactivation of distributed memory traces in primate neocortex. *Science* 297(5589):2070–2073.
9. Kolb B, Whishaw IQ (2001) *An Introduction to Brain and Behavior* (Worth Publishers, New York).
10. Hernández A, Salinas E, García R, Romo R (1997) Discrimination in the sense of flutter: New psychophysical measurements in monkeys. *J Neurosci* 17(16):6391–6400.
11. Lemus L, et al. (2007) Neural correlates of a postponed decision report. *Proc Natl Acad Sci USA* 104(43):17174–17179.
12. Hernández A, et al. (2010) Decoding a perceptual decision process across cortex. *Neuron* 66(2):300–314.
13. Hernández A, et al. (2008) Procedure for recording the simultaneous activity of single neurons distributed across cortical areas during sensory discrimination. *Proc Natl Acad Sci USA* 105(43):16785–16790.
14. Massey J (1990) Causality, feedback and directed information. *Proceedings of the International Symposium on Information Theory and Applications* (ISSTA, Waikiki, HI), pp 303–305.
15. Shannon C, Wiener W (1949) *The Mathematical Theory of Communications* (Univ of Illinois Press, Champaign, IL).
16. Kendall MG (1948) *Rank Correlation Methods* (Griffin, London).
17. Agresti A, Coull BA (1998) Approximate is better than "exact" for interval estimation of binomial proportions. *Am Stat* 52(2):119–126.
18. Victor JD (2005) Spike train metrics. *Curr Opin Neurobiol* 15(5):585–592.
19. de la Rocha J, Doiron B, Shea-Brown E, Josić K, Reyes A (2007) Correlation between neural spike trains increases with firing rate. *Nature* 448(7155):802–806.
20. Cohen MR, Kohn A (2011) Measuring and interpreting neuronal correlations. *Nat Neurosci* 14(7):811–819.
21. Eckhorn R, Thomas U (1993) A new method for the insertion of multiple microprobes into neural and muscular tissue, including fiber electrodes, fine wires, needles and microsensors. *J Neurosci Methods* 49(3):175–179.
22. Jiao J, Permuter H, Zhao L, Kim K, Weissman T (2013) Universal estimation of directed information. *IEEE Trans Inf Theory* 59(10):6220–6242.
23. Willems F, Shtarkov Y, Tjalkens T (1995) The context-tree weighting method: Basic properties. *IEEE Trans Inf Theory* 41(3):653–664.
24. Schreiber T (2000) Measuring information transfer. *Phys Rev Lett* 85(2):461–464.
25. de Lafuente V, Romo R (2006) Neural correlate of subjective sensory experience gradually builds up across cortical areas. *Proc Natl Acad Sci USA* 103(39):14266–14271.
26. Ernst M (2004) Permutation methods: A basis for exact inference. *Stat Sci* 19(4):676–685.
27. Phipson B, Smyth GK (2010) Permutation P-values should never be zero: Calculating exact P-values when permutations are randomly drawn. *Stat Appl Genet Mol Biol* 9:e39.